A Micromachined Photo-Supercapacitor Integrated with CdS-Sensitized Solar Cells and Buckypaper

Fu-Wei Lee, Cheng-Wen Ma, Yu-Hsuan Lin,
Po-Cheng Huang, Yen-Li Su, and Yao-Joe Yang[*]

Department of Mechanical Engineering, National Taiwan University,
No. 1, Sec. 4, Roosevelt Rd., Taipei 10617, Taiwan

In this paper, the development of an all-solid-state photo-supercapacitor (PSC) by micromachining techniques is discussed. The device consists of two ZnO-nanorod solar cells, a buckypaper-based supercapacitor (SC), and an indium tin oxide-coated polyethylene terephthalate substrate. The two solar cells were connected in series by sputtered Au films for scaling up the output voltage. The proposed device is highly flexible, lightweight, and durable. The total photocharge voltage of the PSC exceeded 1.0 V. The energy conversion efficiency of the PSC was 0.26%, and the maximum specific capacitance of the SC was 95.25 F/g. The photocharging–discharging process was measured. Cycle stability measurements showed that 95.89% of the initial specific capacitance was retained after 1000 cycles.

1. Introduction

To alleviate dependence on fossil fuels, many studies have focused on harvesting energy from renewable energy sources, such as wind, hydro, geothermal, and solar energies. Because solar energy is the cleanest and most abundant renewable energy source available, it is the most viable energy source for meeting energy demands and will become crucial in the future. Since the realization of silicon-based solar cells in the 1950s, numerous studies have developed low-cost and high-performance solar cells.[1–3] Typical commercially available solar cells are stand-alone components that must be integrated with other discrete modules (*e.g.*, batteries) for full operation. Such integration usually requires external electrical interconnection, leading to an extra energy loss. Therefore, miniaturized photo-supercapacitors (PSCs), which are realized by monolithically integrating solar cells with supercapacitors (SCs), offer promising energy storage applications, and have received considerable attention in recent years in solar energy industries.[4–6]

In general, according to device structures, PSCs can be categorized into a two-electrode type,[7,8] a three-electrode type,[9] or a core–shell wire type.[10] The three-electrode configuration achieves a higher energy output than does the two-electrode system. Various three-electrode-type PSCs have been reported. Chen *et al*.[11] presented a plastic PSC with a three-layer configuration. The proposed configuration separates a flexible solar cell and an SC by sharing a common platinum electrode. Wee *et al*.[12] created a printable PSC by integrating an organic photovoltaic cell and a carbon-

---

[*]Corresponding author: e-mail: yjy@ntu.edu.tw

nanotube-based SC. A PSC was demonstrated using an N3-dye-adsorbed TiO$_2$ photoelectrode and PProDOT-Et2 polymer films as SC materials.[13] Skunik-Nuckowska *et al.*[14] presented a solid-state PSC integrated with a dye-sensitized solar cell (DSSC) and an electrochemical capacitor. The device could operate under low light intensity conditions. Cohn *et al.*[15] proposed a simple wafer-scale process in which a silicon wafer was used as the central electrode for the anode of a DSSC and an electrode for an electrochemical SC. Bae *et al.*[16] proposed hybrid devices for energy harvesting and storage along a microfiber using ZnO nanorods and graphene. Both mechanical and solar energies were simultaneously scavenged and stored in the devices. In addition, a microfiber that simultaneously achieves photoelectric conversion and energy storage was reported.[17] The proposed device was realized by coaxially integrating a DSSC with an electrochemical capacitor.

In this work, we present a solid-state PSC with a three-electrode configuration by monolithically integrating a buckypaper-based SC with two CdS-sensitized solar cells (CdS-SSCs) and ZnO nanorods. Two CdS-SSCs were connected in series for scaling up the output voltage to increase the output power. The solar cells and SC were monolithically fabricated using micromachining techniques, thus reducing the energy loss between the solar cells and the SC. In addition, the device was realized on an indium tin oxide (ITO)-coated polyethylene terephthalate (PET) substrate, and polyvinyl alcohol–potassium hydroxide (PVA–KOH) was used as the electrolyte. Therefore, the proposed PSC has advantages such as flexibility and simple device packaging. The measured cyclic voltammetry (CV) curves and the photocharging and discharging curves of the device are provided. The rest of the paper is organized as follows: In § 2, the device design and the device fabrication processes, including buckypaper preparation, synthesis of ZnO nanorod arrays, and fabrication of PSC, are presented. In § 3, the measurement results are discussed, and finally, § 4 contains our conclusions.

2. Materials and Methods

2.1 Device design

Figure 1 shows the design of the PSC, which includes two CdS-SSCs and an SC. The entire device was monolithically implemented in-plane on an ITO-coated PET sheet substrate. Interconnect Au was deposited and patterned on top of the device, and the two CdS-SSCs and SC
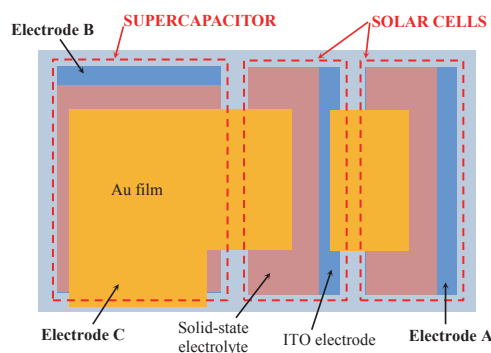

Fig. 1. (Color online) Device configuration of the photo-supercapacitor.

were connected in series for scaling up the output voltage and directly storing the electricity in the SC with a three-electrode configuration. The CdS-SSCs are based on ZnO nanorods and CdS nanoparticles. The oriented crystalline ZnO nanorods are the units for harvesting solar energy. In addition, the CdS nanoparticles serve as a sensitizer of the CdS-SSCs and are deposited on the ZnO nanorod array uniformly. The SC consists of buckypaper electrodes with PVA–KOH gel electrolyte for storing the energy generated by CdS-SSCs.

As shown in Fig. 1, three electrodes were implemented in the device, Electrode A, Electrode B, and Electrode C. When Electrode A and Electrode B are connected, the device is ready to store the energy in the SC. When sunlight radiates on the CdS-SSCs, solar-generated electrons are injected into the conduction band of ZnO nanorods from CdS molecules and are transported to the SC; the generated holes accumulate at the Au electrode. When Electrode B and Electrode C are connected with a load impedance, the energy stored in the SC can be supplied to the load.

ZnO nanorods are relatively durable for solar cell applications.[18] Also, tidy rods of ZnO are advantageous for regulating the movement of charge carriers. Each ZnO nanorod can be considered as an n-type semiconductor with high electron mobility because of single-crystalline morphology. In general, electron transport in a ZnO nanorod is about a few orders of magnitude faster than that of a polycrystalline material.

In addition, because buckypapers are films of paperlike entangled CNT assemblies held together by van der Waals forces, they exhibit excellent properties such as high electrical conductivity, high thermal conductivities, high flexibility, and high mechanical stability.[19] Furthermore, buckypapers have high effective surface areas due to the highly entangled CNT configuration, which is especially advantageous for supercapacitor applications that require large charge capacity.

2.2 Buckypaper preparation

Buckypaper was fabricated by filtering a single-walled carbon nanotube (SWCNT) solution by vacuum filtration. The 0.01 wt% SWCNT solution was completely mixed using an ultrasonic agitator for 2 h to reduce the bundling tendency of the SWCNTs before filtration. The SWCNTs used in this study were 10–20 nm in diameter and 1–2 μm in length (Golden Innovation Business, Taiwan). A nylon membrane filter (MS®) with a pore size of 0.45 μm was used for vacuum filtration. After vacuum filtration, the membrane filter with an SWCNT film was dried at room temperature for 2 h, and the film was subsequently removed. The SWCNT film was a thick free-standing membrane, which is also known as a buckypaper.[20] In this study, the thickness of the buckypaper was approximately 70 μm.

2.3 Synthesis of ZnO nanorod arrays

ZnO nanorod arrays were synthesized using a chemical solution method[21] that involved a simple two-step process. In the first step, ZnO seeds were spin-coated on the top surface of an ITO-PET substrate to form a ZnO crystal seed film (i.e., a seed layer). The process details of growing the ZnO seed layer were described by Greene *et al*.[22] In the second step, ZnO was hydrothermally grown by immersing the ITO-PET substrate upside down in a dish filled with 0.025 M aqueous zinc nitrate hexahydrate, 0.005 M polyethylenimine, and 0.80 M ammonium hydroxide at 95 °C.[23] The reaction continued for 3 h. In this study, the length of the ZnO nanorod was approximately 10 μm. Figure 2 shows the scanning electron microscopy image of the ZnO nanorod arrays.
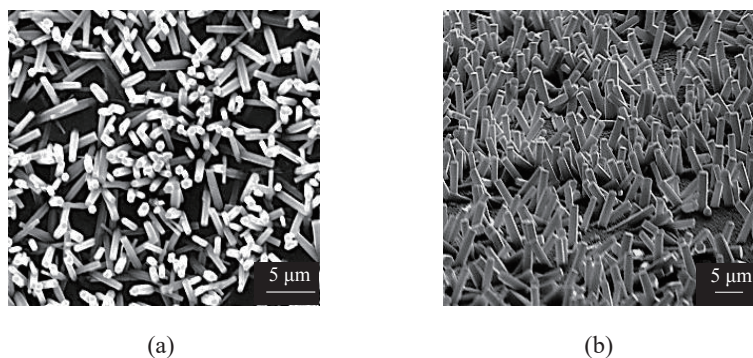
(a)   (b)

Fig. 2.   SEM images of ZnO nanorod arrays: (a) top view and (b) side view.

2.4   Fabrication of PSC

The fabrication process is shown in Fig. 3.   First, the ITO-PET substrate was patterned as three electrodes [Figs. 3(a) and 3(b)].   The texture ZnO seed layer was placed on the substrate and subsequently dried in air [Fig. 3(c)].   The coated substrate was annealed at 150 °C for 20 min to form ZnO nanoparticles (NPs), which were patterned using reactive-ion etching [Fig. 3(d)].   Subsequently, ZnO nanorods were grown, and a CdS sensitizer was coated [Fig. 3(e)].   A chemical bath deposition method was used for embedding CdS NPs at room temperature.[24]   The SC consisted of two SWCNT film electrodes with an identical composition separated by a PVA-KOH electrolyte [Fig. 3(f)].   The electrolyte was dispensed on the ZnO nanorod layer and buckypaper [Fig. (g)].   Finally, a Au film was deposited as an electrode and electrical connection layer [Fig. 3(h)].   The fabricated PSC is shown in Fig. 4.   The size of each solar cell was approximately 5×10 mm^2, and the size of the SC was approximately 10×10 mm^2.

3.   Results and Discussion

Figure 5 shows the current–voltage curves of the solar cell.   Measurements were obtained using a source meter (Keithley 2400).   Simulated AM 1.5G illumination (100 mW/cm^2) was provided using a solar light source (Newport class A), and the light intensity was measured using a calibrated Si solar cell.   The total area of the photoanode for measurement was 0.5 cm^2, and the voltage was scanned from −1 to 1 V with a fixed increment of 0.025 V.   In Fig. 5, the solar cell efficiency, fill factor, open-circuit voltage, and short-circuit current were 0.26%, 0.35, 0.55 V, and 2.0 mAcm^{-2}, respectively.   The CV curves of the fabricated SC at various scan rates (10–200 mV/s) are shown in Fig. 6.   The shape of the CV curves was mirrored with respect to the line of zero current.   Furthermore, the CV curves showed a rapid response to current as the voltage scanning was reversed.   This behavior indicates that the buckypaper SC possesses an electrical double-layer capacitance with small equivalent series resistance and has a high electrochemical reversibility.   Typically, specific capacitance can be evaluated from the measured CV curves using the following equation:[25]

$$C = \frac{AREA_{CV}}{m \cdot s \cdot \Delta V},$$
(1)

(a) ITO-PET film

(b) Patterned ITO

(c) Spin coating of ZnO seed layer

(d) RIE of ZnO NPs

(e) Growing ZnO nanorods and coated CdS sensitizer

(f) Supercapacitor assembly

(g) Electrolyte dispenser

(h) Au film deposited

ITO   ZnO NPs   Electrolyte   Au film
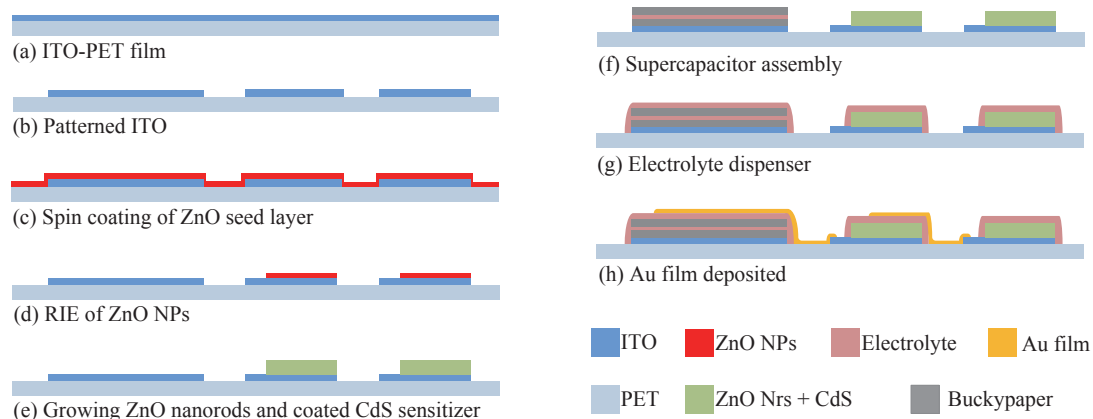
PET   ZnO Nrs + CdS   Buckypaper

Fig. 3.   (Color online) Fabrication process for the PSC.
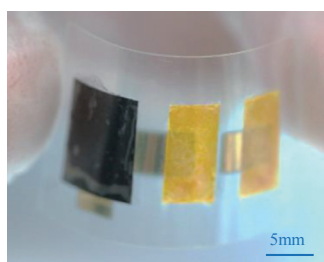
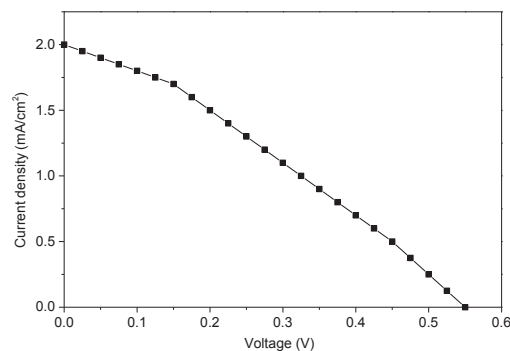Fig. 4. (Color online) Fabricated PSC.

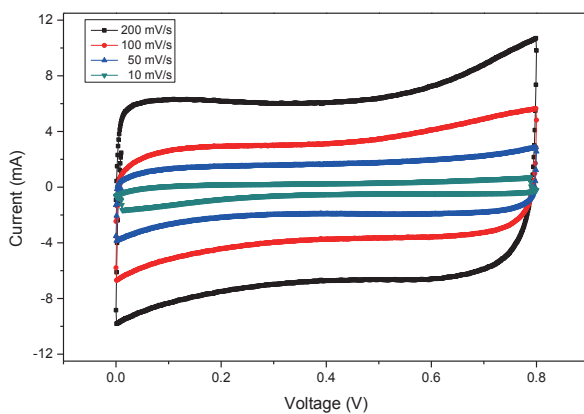Fig. 5.   Measured *I–V* curve of solar cell.

Fig. 6.   (Color online) CV curves of SC at different scan rates.

where $AREA_{CV}$ is the area integral of the voltammogram (i.e., the total voltammetric charge obtained by integrating the positive and negative sweeps in a cyclic voltammogram), s is the scan rate, m is the mass of the electrode, and ΔV is the scanned potential window. The specific capacitance

decreased from 95.25 to 62.5 F/g when the potential scan rate increased from 10 to 200 mV/s. For low scan rates, the *C* values become higher because ions have sufficient time to penetrate and reside in almost all the available pores of the buckypaper electrodes and form electric double layers, which results in higher capacitance. In contrast, at a high scan rate, the ions might not have enough time to penetrate in the available pores of electrodes to form electric double layers, which in turn decreases the capacitance.[26]

Figure 7 shows the plot of the capacitance retention ratio versus the number of repeating CV cycles at a scan rate of 1 V/s. After 1000 cycles, 95.89% of the initial specific capacitance of the device was retained. The inset in the figure shows the CV curves of the first, 250th, 750th, and 1000th cycles. Figure 8(a) shows the plot of voltage versus the time required for photocharging and discharging. During charging, Electrode A and Electrode B were shorted [Fig. 8(b)], and the PSC was charged by illumination under 100 mWcm^{-2} for 200 s. The electrons photogenerated by the solar cells flowed to the SC and were stored in the buckypaper SC. The photovoltage formed on the solar cells was the maximum charging voltage of the SC. The photovoltage increased
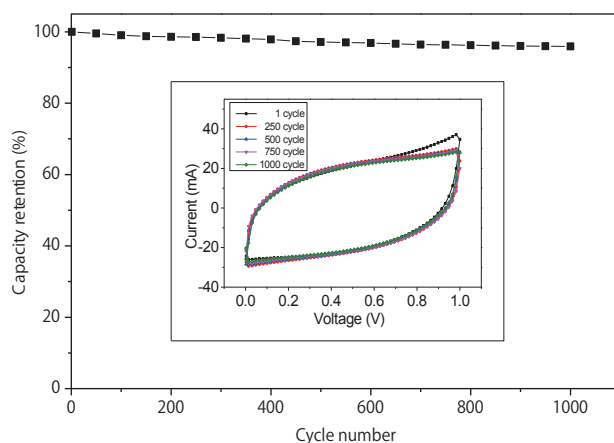

Fig. 7.   (Color online) Cycle stability of micro-SC at a scan rate of 1 V/s. The inset shows the CV curves of the 1st, 250th, 750th, and 1000th cycles.

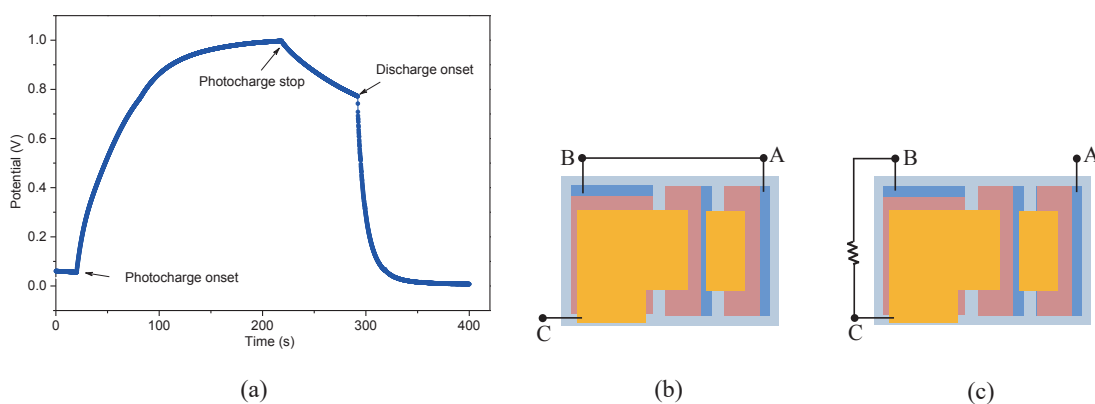| (a) | (b) | (c) |

Fig. 8.   (Color online) (a) Curves of voltage vs time of photocharging and discharging. (b) Configuration for photocharging. (c) Configuration for discharging.

rapidly and reached a maximum of 1 V with 180 s of illumination. After charging for 200 s, the illumination was stopped, and Electrode A and Electrode B were disconnected for 100 s. The voltage of the SC decreased gradually, and a small drop was observed, indicating that the SC self-discharged slowly within 100 s. The SC was then discharged with a loading resistance [Fig. 8(c)]. The voltage rapidly decreased to 0 V as the stored energy dissipated through the resistor via Joule heating. For the proposed device, two CdS-SSCs were designed and connected in series so that the output voltage was scaled up. The experiment results showed that the total photocharge voltage of PSC was approximately 1.0 V, which was higher than that shown in earlier work.[10,12,13] Potentially, the proposed device is more suitable for applications of low-power integrated circuit devices.

4.   Conclusions

In this study, we fabricated a solid-state PSC by integrating a buckypaper-based SC and two CdS-SSCs with ZnO nanorods. Featuring an ITO-coated PET substrate and PVA-KOH electrolyte, the device is flexible, and the packaging process for the device is simple. The experimental results of the PSC, including CV and photocharging–discharging behavior, were presented. The total photocharge voltage of PSC was approximately 1.0 V. The energy conversion efficiency of the PSC was 0.26%, and the maximum specific capacitance of SC was 95.25 F/g. Cycle stability measurements revealed that 95.89% of the initial specific capacitance was retained after 1000 cycles.

Acknowledgements

References

1   M. A. Green, K. Emery, Y. Hishikawa, W. Warta, and E. D. Dunlop: Prog. Photovolt: Res. Appl. **23** (2015) 1.
2   J. You, L. Dou, K. Yoshimura, T. Kato, K. Ohya, T. Moriarty, K. Emery, C.-C. Chen, J. Gao, G. Li, and Y. Yang: Nat. Commun. **4** (2013) 1446.
3   H. Zhou, Q. Chen, G. Li, S. Luo, T.-B. Song, H.-S. Duan, Z. Hong, J. You, Y. Liu, and Y. Yang: Science **345** (2014) 542.
4   T. Miyasaka and T. N. Murakami: Appl. Phys. Lett. **85** (2004) 3932.
5   J. Xu, H. Wu, L. Lu, S.-F. Leung, D. Chen, X. Chen, Z. Fan, G. Shen, and D. Li: Adv. Funct. Mater. **24** (2014) 1840.
6   N. Bagheri, A. Aghaei, M. Y. Ghotbi, E. Marzbanrad, N. Vlachopoulos, L. Häggman, M. Wang, G. Boschloo, A. Hagfeldt, M. Skunik-Nuckowska, and P. J. Kulesza: Electrochim. Acta. **143** (2014) 390.
7   X. Huang, X. Zhang, and H. Jiang: J. Power Sources **248** (2014) 434.
8   X. Zhang, X. Huang, C. Li, and H. Jiang: Adv. Mater. **25** (2013) 4093.
9   T. N. Murakami, N. Kawashima, and T. Miyasaka: Chem. Commun. **14** (2005) 3346.
10   T. Song and B. Sun: ChemSusChem **6** (2013) 408.
11   H.-W. Chen, C.-Y. Hsu, J.-G. Chen, K.-M. Lee, C.-C. Wang, K.-C. Huang, and K.-C. Ho: J. Power Sources **195** (2010) 6225.
12   G. Wee, T. Salim, Y. M. Lam, S. G. Mhaisalkar, and M. Srinivasan: Energy Environ. Sci. **4** (2011) 413.
13   C.-Y. Hsu, H.-W. Chen, K.-M. Lee, C.-W. Hu, and K.-C. Ho: J. Power Sources **195** (2010) 6232.
14   M. Skunik-Nuckowska, K. Grzejszczyk, P. J. Kulesza, L. Yang, N. Vlachopoulos, L. Häggman, E. Johansson, and A. Hagfeldt: J. Power Sources **234** (2013) 91.

15 A. P. Cohn, W. R. Erwin, K. Share, L. Oakes, A. S. Westover, R. E. Carter, R. Bardhan, and C. L. Pint: Nano Lett. **15** (2015) 2727.
16 J. Bae, Y. J. Park, M. Lee, S. N. Cha, Y. J. Choi, C. S. Lee, J. M. Kim, and Z. L. Wang: Adv. Mater. **23** (2011) 3446.
17 X. Chen, H. Sun, Z. Yang, G. Guan, Z. Zhang, L. Qiu, and H. Peng: J. Mater. Chem. A. **2** (2014) 1897.
18 Y. Hames, Z. Alpaslan, A. Kösemen, S. E. San, and Y. Yerli: Sol. Energy **84** (2010) 426.
19 J. Che, P. Chen, and M. B. Chan-Park: J. Mater. Chem. A **1** (2013) 4057.
20 M. Endo, H. Muramatsu, T. Hayashi, Y. A. Kim, M. Terrones, and M. S. Dresselhaus: Nature **433** (2005) 476.
21 L. Vayssieres, K. Keis, S.-E. Lindquist, and A. Hagfeldt: J. Phys. Chem. B **105** (2001) 3350.
22 L. E. Greene, M. Law, J. Goldberger, F. Kim, J. C. Johnson, Y. Zhang, R. J. Saykally, and P. Yang: Angew. Chem. Int. Ed. **42** (2003) 3031.
23 M. Law, L. E. Greene, J. C. Johnson, R. Saykally, and P. Yang: Nat. Mater. **4** (2005) 455.
24 R. S. Mane and C. D. Lokhande: Mater. Chem. Phys. **65** (2000) 1.
25 Y. Jin, H. Chen, M. Chen, N. Liu, and Q. Li: ACS Appl. Mat. Inter. **5** (2013) 3408.
26 R. Farma, M. Deraman, Awitdrus, I. A. Talib, R. Omar, J. G. Manjunatha, M. M. Ishak, N. H. Basri, and B. N. M. Dolah: Int. J. Electrochem. Sci. **8** (2013) 257.